Original Investigation

The Value of Dual Time Point ^{18}F-FDG PET/CT Imaging in Differentiating Lymph Node Metastasis From Reactive Hyperplasia in Bladder Urothelial Carcinoma

Xiang Zhou[1], Zehua Lu[1], Ruixue Zhang[1], Ruiyun Zhang, Gang Huang, Kuangyu Shi, Haige Chen, Jianjun Liu

Rationale and Objectives: This study explored the clinical value of dual time-point ^{18}F-fluorodeoxyglucose (^{18}F-FDG) positron emission tomography (PET) imaging for differentiating lymph node metastasis from lymph nodes with reactive hyperplasia.

Methods: 250 lymph nodes from 153 bladder cancer patients who underwent ^{18}F-FDG PET/computed tomography (CT) delayed diuretic imaging were analyzed. The maximum and mean standardized uptake values (SUVmax and SUVmean, respectively), metabolic tumor volume (MTV), and related delay indices before and after PET delayed imaging were obtained. Relationships with outcomes were analyzed using non-parametric and multivariate analyses. Receiver operating characteristic curves and nomograms were drawn to predict lymph node metastasis.

Results: Delayed PET/CT imaging showed better detection of hyperplasia and metastatic lymph nodes. Delayed imaging with a cutoff SUVmax of 2.0 or 2.5 increased the detection rate of metastatic lymph nodes by 4.1%, and 6.9%, respectively. Delayed imaging often showed speckle-like radioactive foci in lymph nodes with reactive hyperplasia and increased FDG uptake throughout the nodes in metastatic lymph nodes. The lymph node short-axis diameter, SUVmean, and delayed index of MTV (DIMTV) were independent predictors for differentiating metastatic lymph nodes from reactive hyperplasia, and their combination showed better differentiation performance than the individual predictors. In high-risk patients, the probability of lymph node metastasis was as high as 97.6%.

Conclusion: Dual time-point imaging can detect more metastatic lymph nodes. Some lymph nodes with hyperplasia show speckle-like radioactive foci on delayed imaging. The lymph node short-axis diameter, SUVmean, and DIMTV are three important parameters for predicting lymph node metastasis.

Key Words: Lymphatic metastasis; Hyperplasia; Bladder cancer; Positron Emission Tomography Computed Tomography; Fluorodeoxyglucose F18.

INTRODUCTION

Bladder cancer is the most common malignant tumor in the urinary tract, and urothelial carcinoma accounts for 90% of all bladder cancers (1). Abdominal and pelvic lymph nodes are the primary sites of metastases from urothelial carcinoma of the bladder. Metastases in those sites reduces the survival rate by 25 to 31% (2–4). Radical cystectomy and pelvic lymph node dissection are the main

Acad Radiol xxxx; xx:xxx–xxx

From the Department of Nuclear Medicine, Institute of Clinical Nuclear Medicine, Renji Hospital, School of Medicine, Shanghai Jiao Tong University, 1630 Dongfang Rd, Shanghai 200127, China (X.Z., Z.L., G.H., J.L.); Department of Nuclear Medicine, Shanghai Chest Hospital, Shanghai Jiao Tong University, 241 Huaihai West Road, Shanghai 200030, China (R.Z.); Department of Urology, Renji Hospital, School of Medicine, Shanghai Jiao Tong University, 1630 Dongfang Rd, Shanghai 200127, China (R.Z., H.C.); Department of Nuclear Medicine, Inselspital, Bern University Hospital, University of Bern, Street Freiburgstr. 18, Bern 3010, Switzerland (K.S.). Received December 30, 2023; revised February 8, 2024; accepted February 8, 2024. **Address correspondence to**: J.L. e-mail: jianjun_liu2018@163.com

[1] Xiang Zhou, Zehua Lu and Ruixue Zhang contributed equally to this work

https://doi.org/10.1016/j.acra.2024.02.014

treatments for these metastases, and an appropriate extent of lymph node dissection can reduce the incidence of complications while ensuring the therapeutic effect (5). However, accurate preoperative information about lymph node metastasis is crucial for appropriate therapeutic decision-making.

Positron emission tomography/computed tomography (PET/CT) is a functional imaging technique that can simultaneously visualize anatomy and metabolism. The most frequently used tracer for PET/CT imaging is ^{18}F-fluorodeoxyglucose (^{18}F-FDG). PET/CT examinations can detect lymph node metastasis in bladder cancer early, which usually manifests as a nodular radioactive accumulation around the pelvis and abdominal aorta in PET images (6,7). Clinical comparative studies have confirmed that the clinical value of ^{18}F-FDG PET-CT in diagnosing lymph nodes in bladder cancer is higher than those of CT and magnetic resonance imaging (MRI) (8,9). In the 2019 European Association of Urology (EAU) consensus statement on bladder cancer management, 88% of experts endorsed the use of ^{18}F-FDG PET/CT for preoperative evaluation of regional lymph nodes in bladder cancer (10). However, in clinical practice, stimulation of the lymph nodes by bacteria, viruses, and metabolites can induce reactive hyperplasia, enlarged lymph nodes, and/or increased FDG metabolism, which can cause false-positive assessments in PET/CT imaging (11–14). Thus, the accuracy of FDG PET/CT for diagnosing lymph node metastasis needs to be improved further to facilitate appropriate treatment.

Delayed diuretic imaging has been used to locate primary lesions in bladder cancer and has shown some value for differentiation of inflammatory and residual malignant lesions after transurethral resection of bladder tumor (TURBT) (15). Comparisons of changes in lymph node metabolic parameters before and after delayed dual time-point imaging may help distinguish lymph node metastasis from reactive hyperplasia. Therefore, this retrospective study explored the clinical value of delayed FDG PET imaging for differentiation of lymph node metastasis and reactive hyperplasia by analyzing and comparing the FDG PET/CT parameters before and after delayed diuretic imaging.

MATERIALS AND METHODS

Patients and Study Design

The present study retrospectively analyzed 250 lymph nodes in 153 bladder cancer patients from January 2016 to August 2022 (Fig 1). All patients underwent ^{18}F-FDG PET/CT and

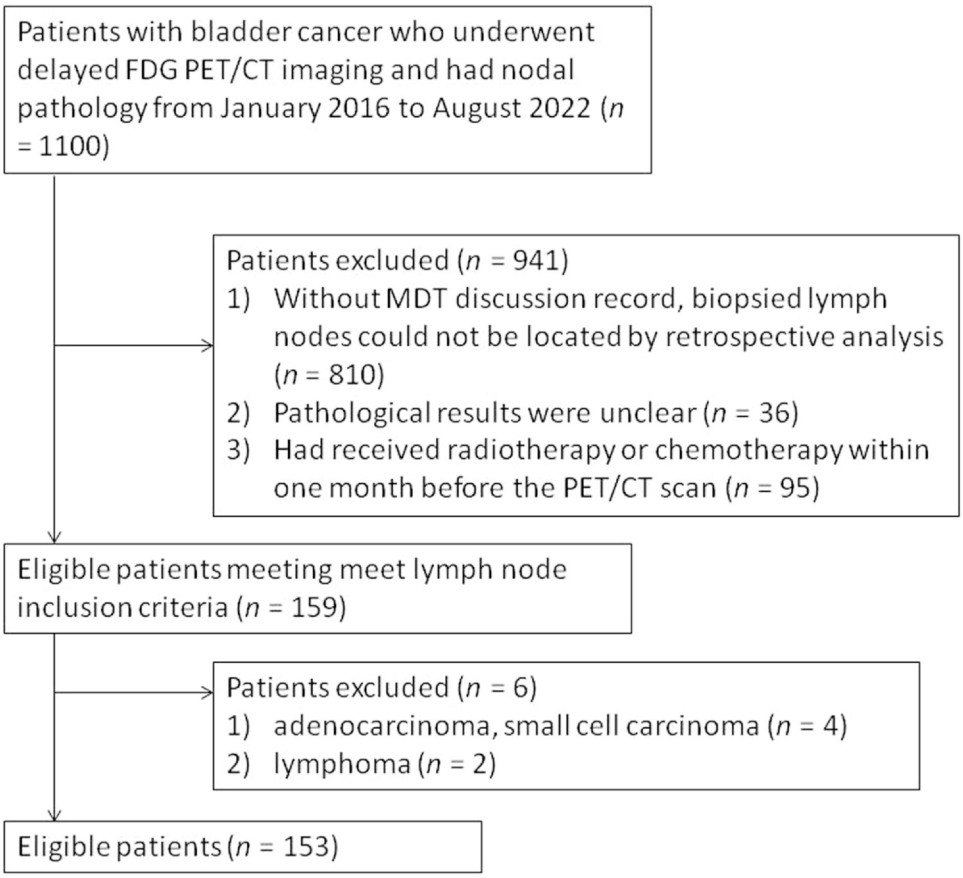

Figure 1. Flowchart showing the study inclusion and exclusion criteria. A total of 153 patients with bladder cancer underwent ^{18}F-FDG PET/CT. After PET/CT, lymph node dissection or lymph node biopsy for bladder cancer was performed within two weeks between January 2016 and April 2021.

lymph node biopsy within two weeks after the PET/CT examination. The lymph node pathology was confirmed by pathological examinations. The study population included cases in which fine-needle aspiration or open abdominal biopsy of the lesion was performed under PET/CT or CT imaging guidance after detailed multidisciplinary team (MDT) discussions, and lymph node pathological results and a clear pathological diagnosis were available. A total of 153 patients met all eligibility criteria and were enrolled in the study. The study design was approved by Ethics Review Board, and all participants provided written informed consent.

^{18}F-FDG PET/CT Acquisition

^{18}F-FDG PET/CT was performed using a PET/CT scanner (Biograph mCT 64; Siemens Medical Systems, Erlangen, Germany). All patients fasted for 6 h before receiving ^{18}F-FDG (0.95% radiochemical purity; Shanghai Kexin Pharmaceutical). The first ^{18}F-FDG PET/CT scan was obtained 50 ± 10 min following intravenous drug administration (3.7 ± 0.37 MBq/kg activity per body weight) with the following parameters: 120 kV; 140 mA; and section thickness, 5.0 mm. PET imaging was performed immediately in 5–6 bed positions after the CT scan (acquisition time, 3 min/bed position). PET raw data were reconstructed using iterative reconstruction with system-specific point spread function modeling and time-of-flight analysis. Projection data were reconstructed with a 5-mm slice thickness (rows, 512; columns, 512; voxel size, 1.5 × 1.5 × 5.0 mm). The patients received oral furosemide 40 mg immediately after the routine first PET/CT scan, drank 1500 mL of water, and urinated several times. At 120 ± 15 min after oral furosemide administration, delayed PET/CT imaging acquisition was performed with 1–2 bed positions in the pelvic district.

^{18}F-FDG PET/CT Image Analysis

All ^{18}F-FDG PET/CT images were reviewed in a workstation (IntelliSpace Portal 7.0; Philips, Amsterdam, the Netherlands) for metabolic parameter measurement and interpreted by two nuclear medicine physicians. The spherical volume of interest (VOI) was delineated using a 40% contour threshold method based on the standardized uptake value (SUV). VOIs were carefully placed in the same anatomical site on both standard and delayed PET/CT scans. SUV was automatically calculated as follows: SUV = tissue radioactivity concentration (MBq/mL) injected dose (MBq)/body weight. The workstation also automatically calculated metabolic parameters before delayed imaging, including maximum uptake value (SUVmax), mean standard uptake value (SUVmean), and metabolic tumor volume (MTV). The corresponding parameters obtained after delayed imaging were named DSUVmax, DSUVmean, and DMTV, respectively, while the corresponding delayed indices were named DISUVmax, DISUVmax, and DIMTV, respectively and calculated as follows (16): DISUVmax = (DSUVmax − SUVmax) × 100/SUVmax; DISUVmean = (DSUVmean − SUVmean) × 100/SUVmean; and DIMTV = (DMTV − MTV) × 100/MTV. The size of suspicious lymph nodes was measured on CT. The calculation of PET/CT parameters, delineation of the region of interest, and visual evaluations were completed by the imaging technology team of the department of Nuclear Medicine of Inselspital at the University of Bern.

Statistical Analysis

Statistical analysis was performed with SPSS software (SPSS, version 16.0; SPSS, Chicago, Ill). Data were presented as mean ± standard deviation. The Mann–Whitney *U* analysis was used to compare the PET metabolic parameters and the lymph node sizes between inflammatory and malignant nodes. Multivariable analyses with logistic regression were performed to identify predictive factors for malignant lymph nodes. Differences in the sensitivity and specificity of each parameter in standard and delayed PET/CT were determined using the chi-square or Fisher's test. On the basis of the associated predictors, the R language nomogram was used to predict lymph node metastasis. A p-value < 0.05 was considered statistically significant.

RESULTS

Study Population and Conventional SUVmax Values for Differentiating Between Lymph Node Metastasis and Reactive Hyperplasia in Bladder Cancer

A total of 153 patients with bladder urothelial carcinoma were included in this retrospective study. The numbers of pT0–T2- and pT3–T4-staged patients were similar. High-grade urothelial carcinoma accounted for 96.73% of the cases ($n = 148$). A total of 250 lymph nodes showed clear pathological findings, including metastatic lymph nodes ($n = 145$, 58%) and reactive hyperplasia ($n = 105$, 42%) **(**Supplement Table 1**)**.

Both metastasis and reactive hyperplasia showed enlarged lymph node volume and increased FDG metabolism (12), making it difficult to diagnose lymph node metastasis by PET/CT. Although SUVmax cutoff values of 2.0 (17) and 2.5 (18,19) have shown high sensitivity for identifying lymph node metastasis in bladder carcinoma, in our study, as shown in Table 1, these cutoff values showed low diagnostic specificity (17.1% and 29.5%, respectively) for identifying lymph node metastasis in bladder urothelial carcinoma and could not effectively differentiate metastatic lymph nodes from lymph nodes showing reactive hyperplasia.

We also analyzed whether delayed ^{18}F-FDG PET/CT imaging could improve the identification of hyperplasia and

TABLE 1. Conventional SUVmax Values in the Lymph Nodes

Parameter	TP	FP	TN	FN	Sensitivity	Specificity
SUVmax						
2.0	138	87	18	7	95.2%	17.1%
2.5	133	74	31	12	91.7%	29.5%
DSUVmax						
2.0	144	94	11	1	99.3%	10.8%
2.5	143	81	24	2	98.6%	22.9%

DSUVmax, maximum uptake value in delayed imaging; FN, false-negative; FP, false-positive; SUVmax, maximum uptake value; TN, true-negative; TP, true-positive

metastasis in lymph nodes (Table 1). A cutoff SUVmax value of 2.0 identified 13 more hyperplastic or metastatic lymph nodes, of which six were identified as metastatic lymph nodes in delayed imaging in comparison with standard imaging; thus, delayed imaging identified 4.1% more metastatic lymph nodes than standard imaging. Similarly, a cutoff SUVmax value of 2.5 identified 17 more hyperplastic or metastatic lymph nodes, of which 10 were identified as metastatic lymph nodes in delayed imaging in comparison with standard imaging; thus, delayed imaging identified 6.9% more metastatic lymph nodes than standard imaging.

Metabolic Parameters for Identifying Lymph Nodes Showing Metastasis and Reactive Hyperplasia in Dual Time-Point Imaging of Bladder Cancer

Since tumors and hyperplasia may differ in the rate of FDG uptake and excretion (14,20), delayed imaging may help differentiate lymph nodes with reactive hyperplasia from lymph node metastases (21,22). However, the changes in metabolic parameters before and after delayed imaging of metastatic lymph nodes and lymph nodes with reactive hyperplasia in bladder cancer have not been studied in detail.

Therefore, we first analyzed dual time-point PET images of lymph nodes showing metastasis and reactive hyperplasia. After delayed imaging, FDG uptake in lymph nodes with reactive hyperplasia tended to gradually aggregate to the central area or other local areas of the lymph node and decreased at the edge of the lymph node, even showing speckle-like or spot foci **(**Fig 2**, case 1, 2)**. However, most of the metastatic lymph nodes showed a persistent increase in FDG uptake throughout the lymph node **(**Fig 2**, case 3, 4)**. Speckle-like foci are more likely in reactive hyperplasia than in metastatic lymph nodes, whereas metastatic lymph nodes are more likely to show globally increased fluorodeoxyglucose uptake in delayed PET/CT imaging.

We further compared the changes in SUVmax, SUVmean, and MTV before and after delayed imaging of metastatic lymph nodes and reactive hyperplasia. The SUVmax and SUVmean in both types of lymph nodes significantly increased after delayed imaging (Fig 3a–c), with 87.6% and 81% of metastatic lymph nodes and lymph nodes with reactive hyperplasia showing increased SUVmax after delayed imaging. Similarly, SUVmean values increased in 77.9% of metastatic lymph nodes and 63.8% of lymph nodes with reactive hyperplasia after delayed imaging (Fig 3a–c). In contrast, while 85.5% of metastatic lymph nodes showed increased MTV values, 61.9% of lymph nodes with hyperplasia showed decreased MTV values after delayed imaging. Thus, the MTV parameters of metastatic lymph nodes increased significantly, while those of lymph nodes with hyperplasia decreased significantly (Fig 3a, d).

Comparison of PET/CT-Related Parameters Before and After Delayed Imaging Between Metastatic Lymph Nodes and Lymph Nodes with Reactive Hyperplasia

We compared the PET/CT-related parameters and analyzed the differences in lymph node length, short-axis diameter, and metabolic parameters in dual time-point imaging between metastatic lymph nodes and lymph nodes showing reactive hyperplasia. Since these data did not show a normal distribution, we used the Mann–Whitney U test to compare the differences between the two groups. All indicators except DISUVmax showed significant differences **(**Supplement Table 2**)**. Multivariable logistic regression analysis to identify the predictive factors for metastatic lymph nodes identified the lymph node short-axis diameter, SUVmean, and DIMTV as independent factors for the diagnosis of lymph node metastasis, among which the DIMTV index was the best parameter for predicting lymph node metastasis **(**Table 2**)**.

Receiver Operating Characteristic Curve and Nomogram Predicted Lymph Node Metastasis

The short-axis lymph node diameter, SUVmean, and DIMTV predicted lymph node metastasis. We also used receiver operating characteristic (ROC) curve analysis to evaluate the usefulness of these parameters and their combination for differentiating between lymph node metastasis and reactive hyperplasia. The results showed that the short-axis lymph node diameter, SUVmean, and DIMTV could distinguish metastatic lymph nodes, and their combination showed an AUC, sensitivity, and specificity of 0.938, 82.8%, and 89.5%, respectively, for predicting lymph node metastasis. Thus, the combination of these indicators allowed

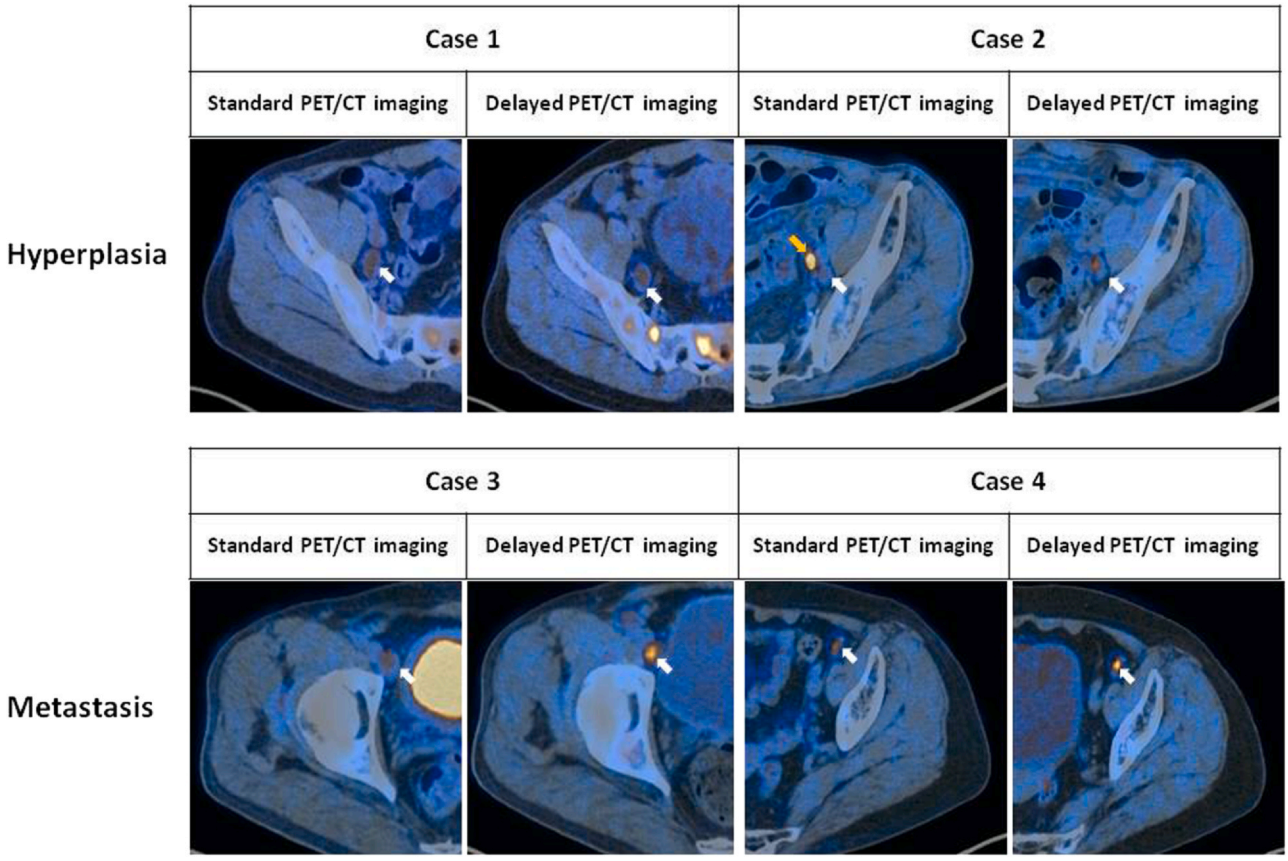

Figure 2. Typical dual time-point PET imaging of reactive hyperplasia and metastatic lymph nodes. After delayed imaging in reactive hyperplasia lymph nodes, some lesions with high FDG metabolism gradually aggregated to the central or other areas of the lymph node and showed a star or spot pattern. The white arrow indicates lymph node reactive hyperplasia in cases 1 and 2. The yellow arrow indicates FDG uptake of the ureter in the standard imaging in case 2. In comparison with standard PET/CT imaging, the pelvic cancerous lymph nodes showed a persistent increase in FDG uptake, and the FDG uptake in the whole lymph node diffusely increased in delayed imaging. The white arrow indicates metastatic lymph nodes in cases 3 and 4. (Color version of figure is available online.)

better prediction of lymph node metastasis than that achieved using a single indicator or a combination of the short-axis diameter and SUVmean (Table 3, Fig 4a). To facilitate more intuitive diagnosis of lymph node metastasis, we drew a nomogram using the short-axis lymph node diameter, SUVmean, and DIMTV to predict lymph node metastasis. DIMTV and SUVmean were more important indicators than the short-axis diameter for predicting lymph node metastasis (Fig 4b).

Differentiation of Lymph Node Metastasis from Lymph Node Inflammatory Hyperplasia by the Combination of the Three Parameters

To facilitate clinical application, we divided the lymph nodes into four groups based on the threshold values for the short-axis diameter, SUVmean, and DIMTV: a high-risk group (short-axis diameter ≥ 7.53, SUVmean ≥ 2.59, and DIMTV ≥ 0.03), a moderate–high-risk group (any two parameters above their cutoff values), a moderate–low-risk group (only one parameter above its cutoff value), and a low-risk group (all three parameters below their cutoff values). The probabilities of lymph node metastasis in these four groups were 97.6%, 75.9%, 36.8%, and 3.6%, respectively, while the probabilities of hyperplasia were 2.4%, 24.1%, 63.2%, 96.4%, respectively. Thus, the rates of metastatic lymph nodes differed significantly among the four risk groups ($P < 0.001$; Table 4).

DISCUSSION

In PET/CT imaging, lymph nodes with reactive hyperplasia are usually enlarged and show increased FDG metabolism, similar to metastatic lymph nodes (12,14). Consequently, reactive nodes cannot easily be distinguished from lymph node metastases, resulting in a high misdiagnosis rate. Since

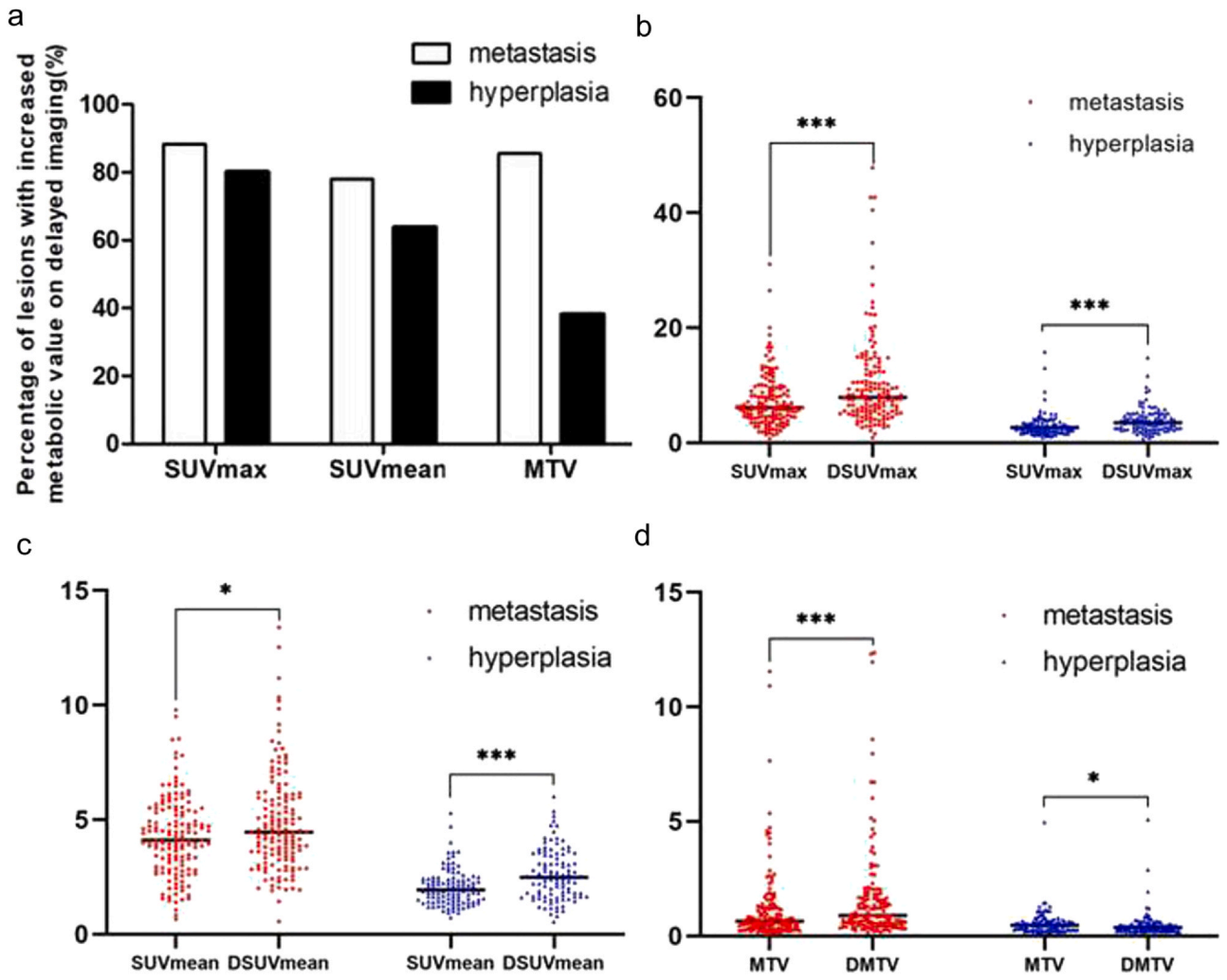

Figure 3. Graphs showing the changes in metabolic parameters in metastatic lymph nodes and reactive hyperplasia after delayed imaging. (**a**) The percentage of lymph nodes showing increased SUVmax, SUVmean, and MTV after delayed imaging in metastatic lymph nodes and reactive hyperplasia. (**b–d**) Comparison of changes in SUVmax, SUVmean, and MTV before and after delayed imaging in metastatic lymph nodes and reactive hyperplasia, respectively. (Color version of figure is available online.)

TABLE 2. Independent Parameters Identified by Stepwise Multivariate Logistic Regression Analysis of Early and Delayed Images for Diagnosing Lymph Node Metastases

Parameters	B	SE	OR	95% CI	P
Short-axis diameters	0.172	0.085	1.188	1.005-1.403	0.027
SUVmean	1.121	0.188	3.069	2.125-4.432	< 0.001
DIMTV	1.445	0.390	4.242	1.976-9.106	< 0.001

CI, confidence interval; DIMTV: delayed index of metabolic tumor volume; OR, odds ratio; SE, standard error; SUVmean, mean standard uptake value.

^{18}F-FDG is mainly excreted by the urinary system and shows a high rate of accumulation in the bladder, furosemide, which can reduce the activity of FDG in the bladder by more than 90%, is used in clinical delayed imaging (15,23).

At our clinical research center, dual time-point PET imaging is routinely performed for diagnosing urinary tract tumors, especially primary bladder cancer. Delayed scanning can avoid the influence of radioactive tracers on the urinary system and more clearly indicate primary bladder cancer and lymph node metastasis near the bladder. Studies have described the usefulness of delayed imaging for diagnosing lymph node metastases in bladder (15), lung cancer (24),

TABLE 3. Comparison of Receiver Operating Characteristic Curves of the Prediction Models for Lymph Node Metastasis

Parameter	AUC	P value	95% CI	Threshold value	Sensitivity	Specificity
Short-axis diameters	0.764	< 0.001	0.706-0.822	7.530	67.6%	73.3%
SUVmean	0.883	< 0.001	0.841-0.925	2.590	83.8%	81.9%
DIMTV	0.832	< 0.001	0.778-0.885	0.032	85.5%	78.1%
Short-axis diameters + DIMTV	0.887	< 0.001	0.846-0.928	0.493	82.1%	83.8%
Short axis diameters + SUVmean + DIMTV	0.938	< 0.001	0.891-0.958	0.530	82.8%	89.5%

AUC, area under the curve; CI, confidence interval; DIMTV, delayed index of metabolic tumor volume; SUVmean, mean standard uptake value

vulvar cancer (16), and breast cancer (25). However, the exact diagnostic mechanism underlying this utility of delayed imaging remains unclear. One possibility is that FDG uptake in hyperplasia or other inflammatory lesions shows a peak followed by rapid FDG excretion while metastatic lymph nodes show continuous uptake or slower excretion of FDG, allowing the differentiation of reactive hyperplasia from metastatic lymph nodes (21).

The use of dual time-point ^{18}F-FDG PET/CT imaging in bladder cancer for differentiation between lymph node metastasis and reactive hyperplasia has not been reported previously. Although several studies have shown that reactive hyperplasia may excrete FDG faster and show a lower SUVmax during delayed imaging while metastatic lymph nodes would continue to take up FDG and thereby show a higher SUVmax, our results indicated that the SUVmax and the SUVmean of both metastatic lymph nodes and reactive hyperplasia increased on delayed imaging after 2 h.

Interestingly, the MTV significantly increased after delayed imaging in most metastatic lymph nodes, whereas it decreased in lymph nodes showing reactive hyperplasia. Image comparisons showed that after delayed imaging, some lymph nodes with reactive hyperplasia showing high FDG metabolism gradually aggregated to the central area of the lymph node, and the FDG uptake at the edge of the lymph node decreased. On delayed FDG imaging, lymph nodes with reactive hyperplasia were more likely to show increased regional FDG uptake than metastatic lymph nodes, whereas metastatic lymph nodes were more likely to show whole, diffuse increased FDG uptake. The mechanism underlying these differences remains unclear, but we speculate that it may be related to the abnormal blood supply to the lymph nodes with hyperplasia. Some investigators have shown that delayed washout distinguishes adrenal metastases from benign adrenal adenomas, which may be the same phenomenon (26–29). During delayed imaging, some lymphocytes in the lymph nodes with reactive hyperplasia can quickly excrete FDG, but because of the abnormalities in blood supply, the FDG transported to these lymph nodes is not rapidly excreted from the entire lymph node but is continuously taken up by lymphocytes in the center of the lymph node. This may explain the increase in the SUVmax observed in the central area of some lymph nodes with reactive hyperplasia and the decrease in the FDG and MTV in the marginal area after delayed imaging. In our study, most cancerous lymph nodes showed a persistent increase in FDG uptake, with a diffuse increase in the FDG uptake in the entire lymph nodes. However, additional evaluations using methods such as autoradiography are required to elucidate the mechanisms underlying these findings. These imaging results can help radiologists visually analyze and identify lymph nodes with reactive hyperplasia and provide imaging and parametric data for artificial intelligence image analysis of lymph nodes with reactive hyperplasia.

We further analyzed the value of metabolic parameters and the related delay indices in differentiating metastatic lymph nodes from reactive hyperplasia and found that the lymph node short-axis diameter, SUVmean, and DIMTV were three independent predictors for differentiating metastatic lymph nodes from reactive hyperplasia. The DIMTV, which is associated with delayed imaging, showed the highest predictive ability for lymph node metastasis, while the short-axis diameter of lymph nodes showed a relatively low predictive ability. The combination of these three predictors yielded an area under the ROC value higher than the individual values of all three factors. We also plotted nomograms and prepared a prediction table of lymph node metastasis risk based on these three parameters. In high-risk patients, the probability of lymph node metastasis and hyperplasia was 97.6% and 3.6%, respectively. Conversely, in low-risk patients, the probability of lymph node metastasis and lymphadenitis was 2.4% and 96.4%, respectively. Thus, the combination of these parameters could facilitate the analysis of pelvic lymph nodes, improving the accuracy of identifying lymph node metastasis and lymph node hyperplasia.

In this study, we used delayed imaging multi-parameter analysis to more accurately distinguish lymph node metastasis from lymph node hyperplasia. Nevertheless, this study had some limitations, including a lack of confirmatory cohort studies and the limitations of delayed imaging itself, such as the increased examination time, long waiting periods for patients, and the increased workload for technicians.

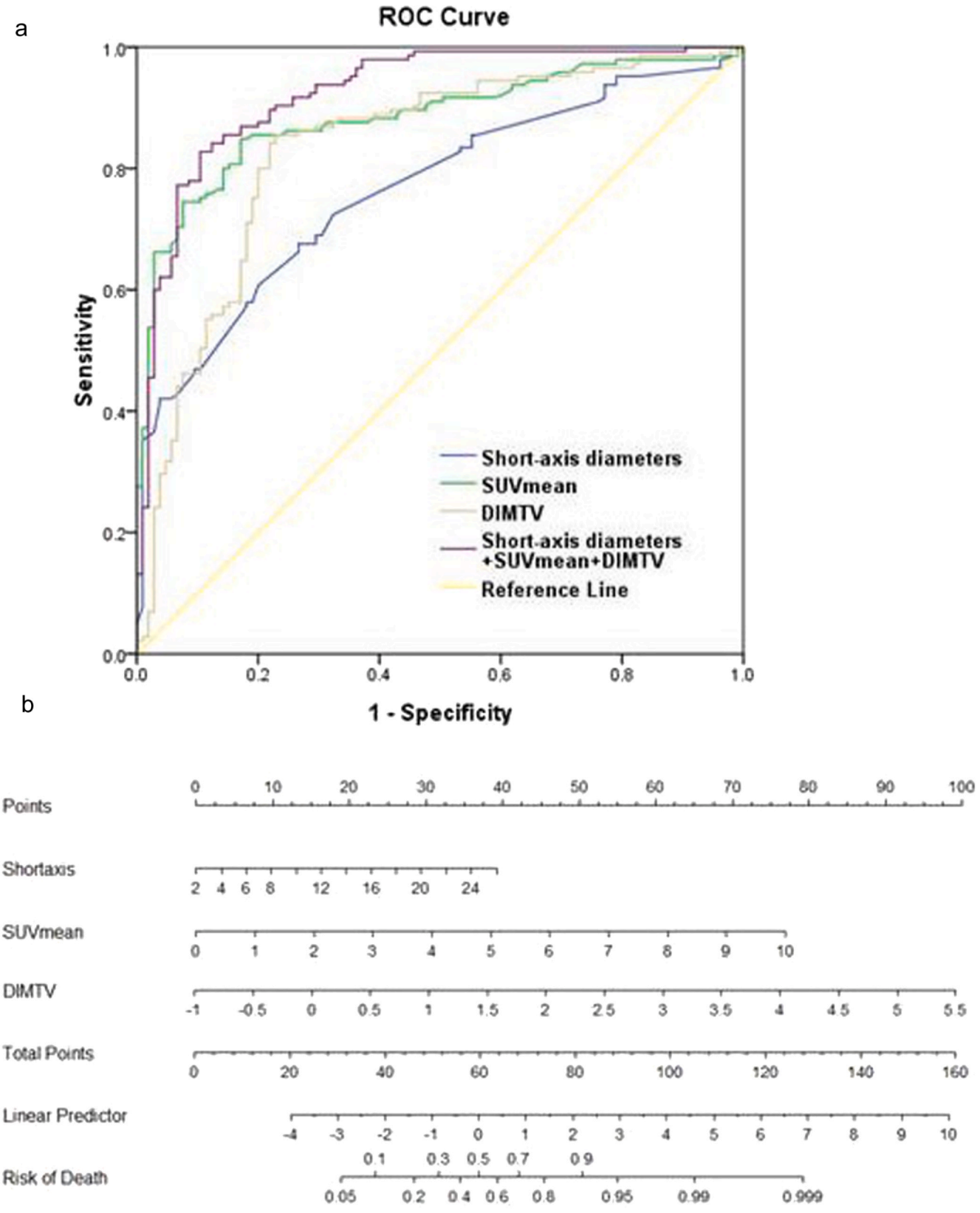

Figure 4. (**a**) ROC curve of the lymph node short-axis diameter, SUVmean, DIMTV, and combined detection for the diagnosis of lymph node metastasis. (**b**) Nomogram for prediction of lymph node metastasis using ^{18}F-FDG PET/CT. The compact model includes the three most relevant predictors (short-axis diameter, SUVmean, DIMTV). For the nomogram, points from the selected clinical variables (top scale) are summed to a total score (lower scale) associated with the estimated probability for ^{18}F-FDG PET/CT positivity. ROC, Receiver operating characteristic. (Color version of figure is available online.)

TABLE 4. Prediction Rate of Metastasis and Hyperplasia in the Lymph Nodes in the High, Moderate–High, Moderate–Low, and Low Risk Groups Categorized by the Combination of These Three Predictors

Group (A)	No. of Lymph Nodes	Probability (%)		P
		Metastasis	Hyperplasia	
High risk	83	97.6%	2.4%	< 0.001
Moderate–High risk	54	75.9%	24.1%	< 0.001
Moderate–Low risk	57	36.8%	63.2%	< 0.001
Low risk	56	3.6%	96.4%	< 0.001

CONCLUSION

In conclusion, delayed imaging can facilitate initial detection of more suspicious lymph nodes. On delayed FDG imaging, lymph nodes with reactive hyperplasia are more likely to show regional FDG uptake than metastatic lymph nodes, whereas metastatic lymph nodes are more likely to show increased global FDG uptake throughout the nodes. Multivariate analysis indicated that the lymph node short-axis diameter, SUVmean, and DIMTV could differentiate between lymph nodes showing reactive hyperplasia and metastatic lymph nodes, and their combination could better differentiate lymph nodes with reactive hyperplasia from lymph node metastases. Thus, the combination of lymph node short-axis diameter, SUVmean, and DIMTV could guide treatment plans in bladder cancer.

DECLARATION OF COMPETING INTEREST

The authors declare that they have no known competing financial interests or personal relationships that could have appeared to influence the work reported in this paper.

ACKNOWLEDGMENTS

Supported by the National Natural Science Foundation of China (81571710, 82171972), the National Key R&D Program of China (2021YFA0910004), and the 5th Three-year Action Program of Shanghai Municipality for Strengthening the Construction of Public Health System (GWV-10.1-XK10). Thanks the Pathology Department of Renji Hospital for supporting this study.

APPENDIX A. SUPPORTING INFORMATION

Supplementary data associated with this article can be found in the online version at doi:10.1016/j.acra.2024.02.014.

REFERENCES

1. Heath EI, Rosenberg JE. The biology and rationale of targeting nectin-4 in urothelial carcinoma. Nat Rev Urol 2021; 18(2):93–103.
2. Karl A, Carroll PR, Gschwend JE, et al. The impact of lymphadenectomy and lymph node metastasis on the outcomes of radical cystectomy for bladder cancer. Eur Urol 2009; 55(4):826–835.
3. Gschwend JE, Dahm P, Fair WR. Disease specific survival as endpoint of outcome for bladder cancer patients following radical cystectomy. Eur Urol 2002; 41(4):440–448.
4. Fleischmann A, Thalmann GN, Markwalder R, et al. Prognostic implications of extracapsular extension of pelvic lymph node metastases in urothelial carcinoma of the bladder. Am J Surg Pathol 2005; 29(1):89–95.
5. Perera M, McGrath S, Sengupta S, et al. Pelvic lymph node dissection during radical cystectomy for muscle-invasive bladder cancer. Nat Rev Urol 2018; 15(11):686–692.
6. Ha HK, Koo PJ, Kim SJ. Diagnostic accuracy of F-18 FDG PET/CT for preoperative lymph node staging in newly diagnosed bladder cancer patients: a systematic review and meta-analysis. Oncology 2018; 95(1):31–38.
7. Soubra A, Hayward D, Dahm P, et al. The diagnostic accuracy of 18F-fluorodeoxyglucose positron emission tomography and computed tomography in staging bladder cancer: a single-institution study and a systematic review with meta-analysis. World J Urol 2016; 34(9):1229–1237.
8. Apolo AB, Riches J, Schoder H, et al. Clinical value of fluorine-18 2-fluoro-2-deoxy-D-glucose positron emission tomography/computed tomography in bladder cancer. J Clin Oncol: Off J Am Soc Clin Oncol 2010; 28(25):3973–3978.
9. Goodfellow H, Viney Z, Hughes P, et al. Role of fluorodeoxyglucose positron emission tomography (FDG PET)-computed tomography (CT) in the staging of bladder cancer. BJU Int 2014; 114(3):389–395.
10. Witjes JA, Babjuk M, Bellmunt J, et al. EAU-ESMO consensus statements on the management of advanced and variant bladder cancer-an international collaborative multistakeholder effort(dagger): under the auspices of the EAU-ESMO guidelines committees. Eur Urol 2020; 77(2):223–250.
11. Makis W, Ciarallo A, Gonzalez-Verdecia M, et al. Systemic lupus erythematosus associated pitfalls on (18)F-FDG PET/CT: reactive follicular hyperplasia, kikuchi-fujimoto disease, inflammation and lymphoid hyperplasia of the spleen mimicking lymphoma. Nucl Med Mol Imaging 2018; 52(1):74–79.
12. Zarzour JG, Galgano S, McConathy J, et al. Lymph node imaging in initial staging of prostate cancer: an overview and update. World J Radiol 2017; 9(10):389–399.
13. Park SA, Lee KM, Choi U, et al. Normal physiologic and benign foci with F-18 FDG avidity on PET/CT in patients with breast cancer. Nucl Med Mol Imaging 2010; 44(4):282–289.
14. Choi EK, Park HL, Yoo IR, et al. The clinical value of F-18 FDG PET/CT in differentiating malignant from benign lesions in pneumoconiosis patients. Eur Radiol 2020; 30(1):442–451.
15. Yan H, Zhou X, Wang X, et al. Delayed (18)F FDG PET/CT imaging in the assessment of residual tumors after transurethral resection of bladder cancer. Radiology 2019; 293(1):144–150.
16. Collarino A, Garganese G, Valdes Olmos RA, et al. Evaluation of dual-timepoint (18)F-FDG PET/CT imaging for lymph node staging in vulvar cancer. J Nucl Med: Off Publ, Soc Nucl Med 2017; 58(12):1913–1918.
17. Girard A, Rouanne M, Taconet S, et al. Integrated analysis of (18)F-FDG PET/CT improves preoperative lymph node staging for patients with invasive bladder cancer. Eur Radiol 2019; 29(8):4286–4293.

18. Jeong IG, Hong S, You D, et al. FDG PET-CT for lymph node staging of bladder cancer: a prospective study of patients with extended pelvic lymphadenectomy. Ann Surg Oncol 2015; 22(9):3150–3156.
19. Aljabery F, Lindblom G, Skoog S, et al. PET/CT versus conventional CT for detection of lymph node metastases in patients with locally advanced bladder cancer. BMC Urol 2015; 15:87.
20. Yao Y, Li YM, He ZX, et al. Likely common role of hypoxia in driving (18) F-FDG uptake in cancer, myocardial ischemia, inflammation and infection. Cancer Biother Radiopharm 2021; 36(8):624–631.
21. Zhou J, Zou S, Cheng S, et al. Correlation between dual-time-point FDG PET and tumor microenvironment immune types in non-small cell lung cancer. Front Oncol 2021; 11:559623.
22. Zhuang H, Pourdehnad M, Lambright ES, et al. Dual time point 18F-FDG PET imaging for differentiating malignant from inflammatory processes. J Nucl Med 2001; 42(9):1412–1417.
23. Nayak B, Dogra PN, Naswa N, et al. Diuretic 18F-FDG PET/CT imaging for detection and locoregional staging of urinary bladder cancer: prospective evaluation of a novel technique. Eur J Nucl Med Mol Imaging 2013; 40(3):386–393.
24. Shinya T, Rai K, Okumura Y, et al. Dual-time-point F-18 FDG PET/CT for evaluation of intrathoracic lymph nodes in patients with non-small cell lung cancer. Clin Nucl Med 2009; 34(4):216–221.
25. Sasada S, Masumoto N, Suzuki E, et al. Prediction of biological characteristics of breast cancer using dual-phase FDG PET/CT. Eur J Nucl Med Mol Imaging 2019; 46(4):831–837.
26. Dunnick NR, Korobkin M, Francis I. Adrenal radiology: distinguishing benign from malignant adrenal masses. Am J Roentgenol 1996; 167(4):861–867.
27. Korobkin M, Brodeur FJ, Yutzy GG, et al. Differentiation of adrenal adenomas from nonadenomas using CT attenuation values. Am J Roentgenol 1996; 166(3):531–536.
28. Korobkin M, Brodeur FJ, Francis IR, et al. CT time-attenuation washout curves of adrenal adenomas and nonadenomas. Am J Roentgenol 1998; 170(3):747–752.
29. Korobkin M, Brodeur FJ, Francis IR, et al. Delayed enhanced CT for differentiation of benign from malignant adrenal masses. Radiology 1996; 200(3):737–742.